



HAL
open science

Biogenic volatile organic compound emissions in central Africa during the Experiment for the Regional Sources and Sinks of Oxidants (EXPRESSO) biomass burning season

J P Greenberg, A B Guenther, S Madronich, W Baugh, A Druilhet, R Delmas, Claire Delon

► To cite this version:

J P Greenberg, A B Guenther, S Madronich, W Baugh, A Druilhet, et al.. Biogenic volatile organic compound emissions in central Africa during the Experiment for the Regional Sources and Sinks of Oxidants (EXPRESSO) biomass burning season. *Journal of Geophysical Research: Atmospheres*, 1999. hal-03026483

HAL Id: hal-03026483

<https://hal.science/hal-03026483v1>

Submitted on 26 Nov 2020

HAL is a multi-disciplinary open access archive for the deposit and dissemination of scientific research documents, whether they are published or not. The documents may come from teaching and research institutions in France or abroad, or from public or private research centers.

L'archive ouverte pluridisciplinaire **HAL**, est destinée au dépôt et à la diffusion de documents scientifiques de niveau recherche, publiés ou non, émanant des établissements d'enseignement et de recherche français ou étrangers, des laboratoires publics ou privés.

Biogenic volatile organic compound emissions in central Africa during the Experiment for the Regional Sources and Sinks of Oxidants (EXPRESSO) biomass burning season

J.P. Greenberg, A.B. Guenther, S. Madronich, and W. Baugh

National Center for Atmospheric Research, Boulder, Colorado

P. Ginoux

NASA Goddard Space Flight Center, Greenbelt, Maryland

A. Druilhet, R. Delmas, and C. Delon

Laboratoire d'Aerologie, Toulouse, France

Abstract. The recent aircraft and ground-based Experiment for the Regional Sources and Sinks of Oxidants (EXPRESSO) campaign in central Africa studied atmospheric trace gases and aerosols during the biomass burning season. Isoprene, emitted from vegetation, was the most abundant nonmethane hydrocarbon observed over the forest and savanna, even though intense biomass burning activity was occurring several hundred kilometers to the north. The isoprene flux, measured directly from midmorning to noon by a relaxed eddy accumulation technique, was approximately $890 \mu\text{g isoprene m}^{-2} \text{h}^{-1}$ from the tropical rain forest and semideciduous forest landscapes and $570 \mu\text{g isoprene m}^{-2} \text{h}^{-1}$ from transitional and degraded woodland landscapes. Model estimates derived from satellite landscape characterization coupled with leaf enclosure emission measurements conducted during EXPRESSO compared well with these measured fluxes. Isoprene concentrations and fluxes were used to determine the oxidant balance over the forest and savanna. Radiative transfer calculations indicate that the observed strong vertical gradient of the NO_2 photolysis rate coefficient could be explained by the presence of substantial amounts of absorbing aerosols, probably from biomass burning. Chemical (box) model simulations of the planetary boundary layer (PBL), constrained by measured isoprene emission fluxes and concentrations, show that this suppression of photolytic radiation lowers OH concentrations by about a factor of 2 relative to aerosol-free conditions. Consequently, the direct contribution of PBL photochemistry to ozone production, especially from biogenic isoprene, is small.

1. Introduction

The tropics contain 40% of the global land area and account for about 60% of the global annual net primary productivity [Rodin *et al.*, 1975]. The diversity of vegetation species in the tropics is far greater than that found at other latitudes. Tropical forest and savanna landscapes, however, are being converted to agricultural uses and pastures at about 1% per year. Biomass burning in the tropics (largely by humans) is primarily responsible for this conversion and has been shown to exert a dominant influence on the ecology and the atmospheric chemistry of most of the tropics [Crutzen and Andreae, 1990]. Biomass burning releases huge amounts of CO , nonmethane hydrocarbons (NMHCs), NO_x , etc. Satellite observations over 5 years indicate that 70% of all biomass burning occurs in tropical areas, half of that in Africa [Dwyer *et al.*, 1998]. The seasonality of African climate results in different burning periods for northern and

southern Africa, with, on average, more burning occurring annually north of the equator [Hao and Liu, 1994].

The biosphere in tropical savannas and forests also releases large quantities of hydrocarbons [Guenther *et al.*, 1995; Brasseur *et al.*, 1999]. Considerable effort has been devoted to characterizing biogenic hydrocarbon emissions in the temperate regions of North America and Europe, with a good deal of success. However, the extremely high species diversity in poorly characterized tropical landscapes, as well as few measurements of biogenic emissions in tropical regions [Zimmerman *et al.*, 1988; Guenther *et al.*, 1996; Klinger *et al.*, 1998], has resulted in highly uncertain estimates for biogenic emissions in the tropics.

Emissions from biomass burning and the products of their photochemistry have been shown to reach the tropical forest [Andreae *et al.*, 1992; Cachier and Ducret, 1991]. Chemical interactions of biomass burning and biogenic emissions north of the equator in Africa are potentially large and may lead to enhanced levels of O_3 in the lower atmosphere [Lopez *et al.*, 1992]. In particular, at the Intertropical Convergence Zone (ITCZ), air (polluted with biomass burning emissions) from the savanna to the north may potentially mix with relatively clean air (with strong biosphere emission influence) from forests and

Copyright 1999 by the American Geophysical Union.

Paper number 1999JD900475.
0148-0227/99/1999JD900475\$09.00

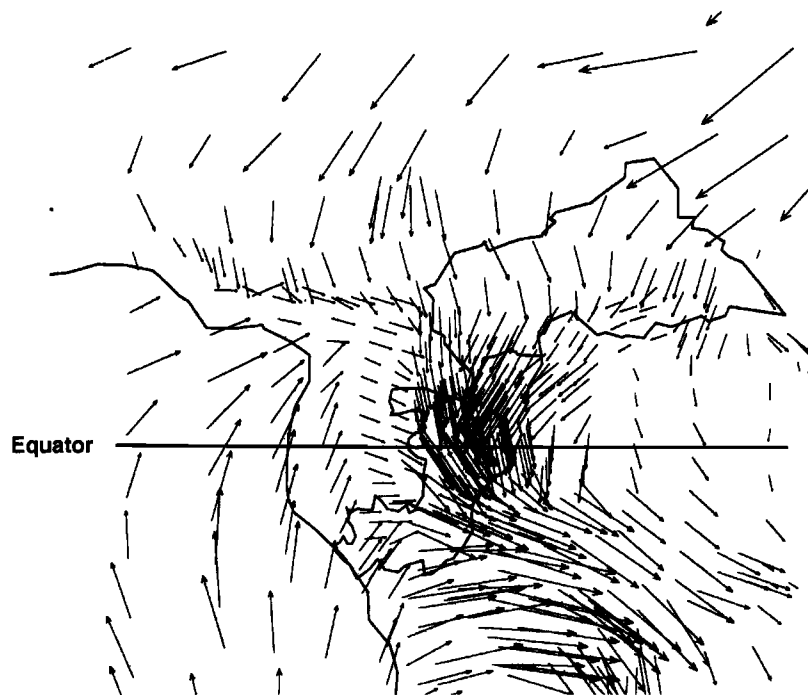
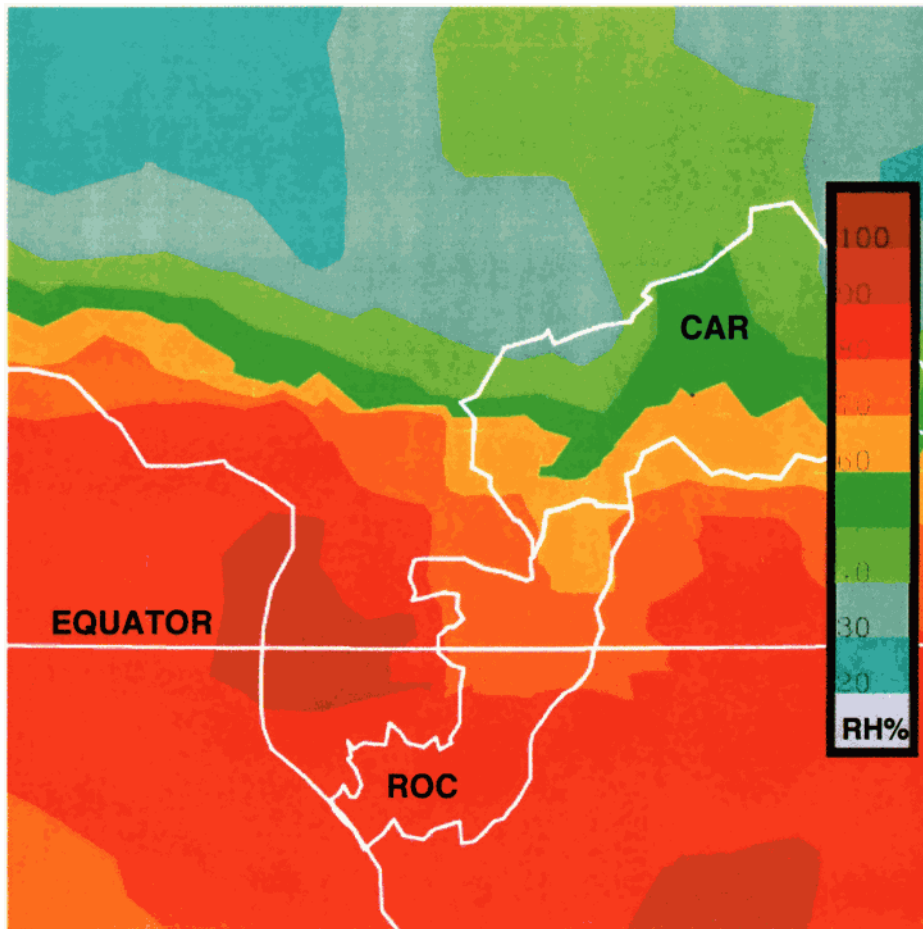


Plate 1(a). Relative humidity (RH) gradient and (b) winds near the surface (950 mbar) in the EXPRESSO region of the Central African Republic (CAR) and the Republic of Congo (ROC) on November 29, 1996, showing the ITCZ and the extensive mixing between monsoon (Southern Hemisphere) and Harmattan (Northern Hemisphere) airflow. A similar scenario existed over the EXPRESSO experimental period. RH and winds are produced from European Centre for Median – Range Weather Forecasts (ECMWF) global troposphere analysis.

savanna-forest mosaics, coming in from the south. In addition, mass flow from the Hadley circulation may lift the converging air through the troposphere, up to 100-200 mbar, where this mixture may also be transported over long distances (Figure 1). The continuing chemical reaction of biomass burning and biogenic trace gases emitted into this circulation may, therefore, have long-range consequences.

The Experiment for the Regional Sources and Sinks of Oxidants (EXPRESSO) investigated processes controlling chemical composition of the tropical troposphere above central Africa and their potential impact on the global atmosphere. The study area of the campaign was in the region of the ITCZ, from the savannas of the Central African Republic (CAR) to the tropical forests of the Republic of the Congo (Congo). Aircraft experiments (November and December 1996) were designed to determine the contributions of biomass burning and biogenic emissions to the chemistry above central African forest and savanna landscapes. These flights originated in Bangui, the capital of CAR (4°24'N 18°31'E). This paper characterizes the numerous nonmethane hydrocarbons (NMHCs) from fires and the biosphere and relaxed eddy accumulation (REA) direct flux measurements of isoprene from savanna and forest landscapes. Chemistry of biomass burning and biogenic emissions in the boundary layer is presented, incorporating the results of other measurements (O₃, NO, NO_x, J_{NO₂}, CO, and a suite of aerosol measurements, etc.) made during the EXPRESSO aircraft campaign by other investigators. The net production of O₃ in the boundary layer over forest and savanna landscapes is estimated. A complete overview of EXPRESSO is presented by *Delmas et al.* [this issue].

2. Experimental Details

2.1. Experimental Region

The EXPRESSO aircraft measurements in the CAR and Congo were made in the vicinity of the ITCZ. Here, the monsoon layer of moist, southwesterly air, originating over the South Atlantic and passing over the tropical rain forest, is overridden by a dry, northeasterly Harmattan flow from the arid areas of northern Africa (Figure 1). At the ITCZ the monsoon layer is several hundred meters thick. In September the ITCZ reaches its northernmost position (20°N). For the northern part of the Congo and southern CAR, this corresponds to the peak of the wet season. In October the ITCZ moves southward, toward its southernmost position (8°N) in January. The main dry season for the EXPRESSO area occurs from December to February, when the ITCZ is located near its southernmost position.

The amount of annual rainfall and the length of the dry period determine the type of vegetation. Rainfall is maximal and most evenly distributed from 4°S to 4°N; the region is dominated by tropical evergreen, seasonal, and edaphic forest. To the north, annual rainfall progressively decreases and the duration and intensity of the dry season increase; largely evergreen forest gradually gives way to forest with a larger deciduous component, then to woodland and dry savanna. Much of the transition between forest and savanna was formerly continuous rain forest. The savanna woodlands are particularly influenced by human activity, with large areas burned each year during the dry season.

During the November-December 1996 EXPRESSO experiment, evidence of significant mixing between the monsoon and Harmattan layers was observed. A relative humidity gradient (30-40% in the northern CAR and 80-90% in the Congo)

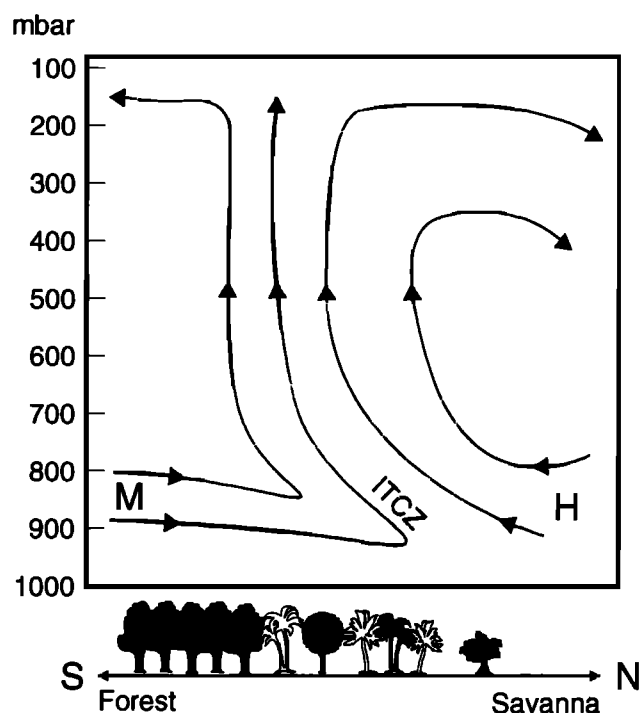


Figure 1. Schematic of the general atmospheric dynamics in central Africa, depicting the Intertropical Convergence Zone (ITCZ), monsoon flow (M) and Harmattan flow (H) in the EXPRESSO region.

extended over 400 km through the study area. Plates 1a and 1b show the relative humidity gradient and surface winds in the region during this period. Biomass burning activity, monitored by satellite, varied during the course of the November-December experiment (P. A. Brivio et al., unpublished manuscript, 1999). More intense burning activity, which potentially impacted the study region, occurred toward the beginning of the experiment, but was usually more than 400 km distant (Cameroon, Chad, Sudan, Zaire). Fires closer to Bangui occurred less frequently and were generally not as intense. Using Bangui as the endpoint, 4-day trajectory analyses at 850 mbar were northerly (originating in southern Sudan and Chad), while 500-mbar trajectories were generally from distant areas in northern and western Africa [*Delmas et al.*, this issue].

2.2 Sampling of Volatile Organic Compounds (VOCs)

2.2.1. Sample collection. Air samples were collected onto solid adsorbent cartridges for the characterization of VOCs in the study region. The cartridges were a three-stage combination (from weakest to strongest adsorbent) of glass beads, Carbotrap®, and Carbosieve S-III® (sold under tradename Carbotrap 200® by Supelco, Inc., Bellefonte, Pennsylvania). This formulation was suitable for the determination of NMHCs in the C₃ – C₁₂ mass range. At aircraft collection temperatures (25°-35°C), the retention volume of propane and propene may have been exceeded, so that their concentrations reported here may be as much as 20% higher in some cases.

Cartridges were stored at approximately –30°C before and after flights, except during transport to and from the Central African Republic. During transport the cartridges were kept in an ice chest (0°-5°C); transport times were approximately 30 hours.

Samples were analyzed by gas chromatography with flame ionization and atomic emission detectors for quantitation and mass spectrometry for peak identifications. Details of the analytical procedures and techniques have been presented earlier [Greenberg *et al.*, 1994, 1996, 1999].

2.2.2. Whole air sampling. Samples were collected by an automated cartridge collection system. Eight cartridges were installed onto the system immediately before flights and removed immediately after flights. Cartridges were isolated on the sampler until the time of sampling. Sample flows were set at 300 mL min⁻¹ by a mass flow controller. All tubing routing sample air to the cartridge was stainless steel and was heated to approximately 70°C. The sampling sequence was commenced manually when the aircraft entered the research areas. Sample flows were recorded continuously, and the cartridge sampling sequence was controlled by a minicomputer/data logger. Seven cartridges were sampled during the flight; the eighth was used as a system blank for each flight. Typical sample volumes for the whole air samples were 3 to 4.5 L.

A separate system was used for the relaxed eddy accumulation (REA) flux measurements. The REA technique segregates air in upward or downward moving eddies into separate reservoirs; the air in the reservoirs is later sampled to determine the concentration of trace gases. The flux of the trace gas is computed from the difference in the concentration between the two reservoirs, the variance of the vertical wind about the mean value, and a constant associated with atmospheric stability. The REA system has been described separately (C. Delon *et al.*, unpublished manuscript, 1999); parameters of REA sampling, including up and down eddy sample switching frequency (10 Hz), vertical velocity threshold ($0.1\sigma_w$), sampling time lag (0.1 s), low-frequency vertical wind filter (0.02 Hz), etc., were assigned from simulations and empirical data.

A gust probe installed on the boom of the aircraft measured fast vertical and horizontal winds. True vertical wind speed was computed by subtracting the vertical motion of the aircraft, measured by the inertial navigation system, from that measured by the gust probe. Air was continuously pumped at a constant flow rate from an inlet on the boom and the flow was diverted to up or down eddy sampling lines, which led to the REA bag

collection system inside the aircraft, or to a vent position when there was no sampling. The REA collection system consisted of up and down eddy Tedlar® bags and a pumping system used to evacuate the bags between samples. REA samples were collected over a constant altitude path length of approximately 30 km; the sampling distance was sufficient to sample the spectrum of eddies observed in the boundary layer [Lenschow, 1975]. After sample collection, CO₂ from each bag was measured in situ and VOCs samples (approximately 900 mL) were collected from the up and down eddy reservoirs. Samples were collected onto Carbotrap 200® solid adsorbent cartridges (described above). Up to five REA sample pairs were collected on each flight. At least one unsampled cartridge pair on each flight was used for analytical blanks.

2.2.3. Locations of sample collection. Whole air and REA samples were collected over the CAR and the Congo during nine flights between November 24 and December 2, 1996. Flight altitudes ranged from approximately 100 m to 4000 m above ground level. Three flights focused over transitional woodland/savanna areas (two near Boali, 4.5°N, 18°E) and another four flights over the tropical forest (three near Enyele, 3°N, 18°E). One flight flew south over the forest-savanna interface; another flew north over the savanna, toward the biomass burning in northeastern CAR and southern Sudan. An additional flight flew south to the region near Bomassa, Congo, where a 65-m walkup tower was constructed for the EXPRESSO experiment (D. Serca *et al.*, unpublished manuscript, 1999).

Whole air sample collection was over 10-15 min, so that the concentrations were integrated over a large spatial extent (50-100 km). There was no large-scale burning in the aircraft study area. Most flights took place during the morning (0930 to 1200 local time), in order to avoid afternoon thunderstorm activity. Flight parameters are given in Table 1.

Most REA flux samples were collected over a 30 km x 30 km expanse of transitional (degraded) woodland (12 flux measurements) near Boali in the CAR and a larger plot over the tropical forest (nine flux measurements) near Enyele in the northernmost part of the Congo (Plate 2). An additional eight measurements were made over other forest and woodland areas within 250 km of Bangui.

Table 1. EXPRESSO Aircraft Flight Details

Date	Time Range	Landscape	Z, ^a	BL ^b	FT ^c
Nov 24	0948-1100	Boali savanna	380	5	2
Nov 25	0937-1047	Enyele forest	400	7	0
Nov 26	0943-1053	Enyele forest	500	7	0
Nov 27	1109-1220	savanna transect	460	4	3
Nov 28	1008-1118	Enyele forest	430	6	1
Nov 29	0941-1051	forest transect	360	3	4
Nov 30	1022-1132	Boali savanna	675	5	2
Dec. 1	0938-1050	Enyele forest	600	7	0
Dec. 2	0856-1006	forest-savanna	150	2	5

^aAverage height of boundary layer during flight

^bNumber of boundary layer samples.

^cNumber of free troposphere samples.

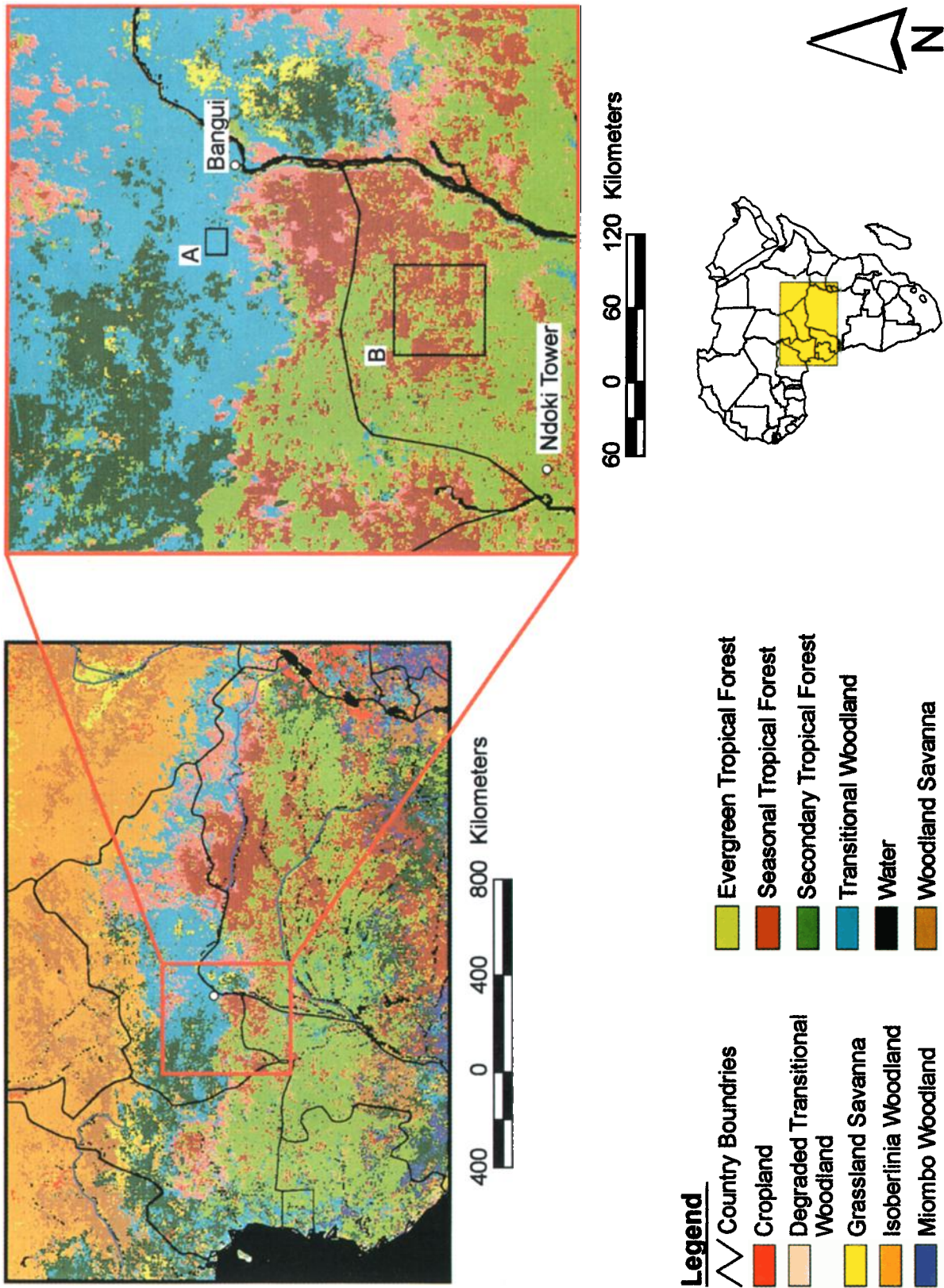


Plate 2. Landscapes in EXPRESSO domain, from advanced very high resolution radiometer (AVHRR) satellite images, with land cover classifications from U.S. Geological Survey EROS Data Center. Aircraft missions (originating in Bangui, Central African Republic) focused on two areas, the Boali woodland-savanna (A) and the Enyele rain forest (B).

2.3. Atmospheric Chemistry Model.

A zero-dimensional (0-D or box) photochemical model was used to examine the chemical interaction of fire emission products, VOCs, and biogenic isoprene in the boundary layer over the forest and savanna. The chemical mechanism consisted of about 3340 gas phase reactions among approximately, 1250 explicit species, as described by *Madronich and Calvert* [1990] and updated by *Aumont et al.* [1999]. Photolysis rates were calculated with the tropospheric ultraviolet-visible (TUV) model [*Madronich and Flocke*, 1998] for late November, 0.5 km above a surface of 5% albedo, and climatological total O₃ column of 260 Dobson units (DU, equal to 2.69x10¹⁹ molecules cm⁻²). Absorption and scattering by aerosols was considered (see below). Time integration of the chemical rate equations was started at midnight with the initial conditions given in Table 2 and was carried out for 2 days, the first of which is considered as a model spin-up period, with results (see below) reported from the second day.

The height of the planetary boundary layer (PBL) was taken as 0.1 km at night, growing linearly to 1.0 km (savanna) or 0.7 km (forest) between 0800 (local time) and 1400; remaining at this maximum value until 1600; then decreasing linearly to reach again the nighttime value at 1800. During the growth of the PBL (0800-1400), the rate of entrainment of air which in the previous time step was just above the PBL is represented as a first-order source or sink for chemical species in the PBL, for example, for species *x*,

$$(dX_{\text{PBL}}/dt)_{\text{entrainment}} = -K_{\text{entrainment}}(X_{\text{PBL}} - X_{bg})$$

where X_{PBL} is the concentration of the species in the PBL, and X_{bg} is the concentration above the PBL (free tropospheric background). The first-order rate constant $K_{\text{entrainment}}$ is estimated from the rate of growth of the PBL height as 6.4x10⁻⁵ s⁻¹ (forest) and 1.1x10⁻⁴ s⁻¹ (savanna) during 0800-1400, and is zero at all other times. Values of X_{bg} were assumed constant with time, and were set to zero for all VOCs (corresponding to simple dilution of PBL air), except for those listed in Table 2, for which measurements above the PBL were available from aircraft flights during EXPRESSO; otherwise, a reasonable climatological estimate was made.

Emissions of isoprene and NO were included and were assumed to be time dependent. For isoprene, emissions (from REA flux measurements) were taken as zero at night (1800 to 0600), increasing linearly to 700 μg C m⁻² h⁻¹ (savanna) or 1200 μg C m⁻² h⁻¹ (forest) (see below), remaining at this level until 1600, and then decreasing linearly to 1800. For NO a similar time dependence was assumed, but from a minimum nighttime value of 10⁵ molecules cm⁻² s⁻¹ to a maximum of 10⁶ molecules cm⁻² s⁻¹, corresponding approximately to the middle of the values considered by *Lopez et al.* [1992]. Deposition of reactive species was parameterized using the resistance-in-series method of *Wesely* [1989], with maximum deposition velocity of 3 cm s⁻¹ for radicals and HNO₃ (zero surface resistance). For nonradical organics, surface resistance was estimated based on reactive moieties (e.g., aldehyde or alcohol groups). In the 0-D model, surface emissions and surface deposition velocities were transformed into effective zero-order and first-order rate constants (respectively) into the PBL volume, and thus were scaled with the inverse of the PBL height.

3. Results and Discussion

3.1. VOC Concentrations

Median (and interquartile range) mixing ratios over the various landscapes are shown in Figure 2. Median values are reported, since observations are not normally distributed; interquartile ranges include the central 50% of the measured mixing ratios. For most NMHCs, except those which are primarily biogenic emissions (isoprene and α-pinene), the mixing ratios are slightly higher over the savanna than over the forest. Except for biogenic emissions, the differences in the concentrations of most NMHCs in the boundary layer and free troposphere over each region were small. Isoprene and α-pinene are much higher in the boundary layer over the forest than over the savanna.

The scale and extent of mixing, indicated by the relative humidity gradient (Plate 1a), were also shown by the mixing ratios of VOCs (Figure 2) and CO [*Delmas et al.*, this issue]

Table 2. Initial Conditions and Background (Free Troposphere) Concentrations Species for Zero-Dimensional Model Simulations

	Concentration			
	Forest		Savanna	
	PBL	Background	PBL	Background
CO ₂ , ppm	350			
H ₂ , ppm	0	6		
CH ₄ , ppm	1	7		
	Concentration			
	Forest		Savanna	
	PBL	Background	PBL	Background
O ₃ ^a , ppb	30	50	35	60
NO ₂ ^b , ppb	1.6	1.0	2.2	1.5
CO ^c , ppb	285	290	300	300

For H₂O, relative humidity is 50%. For nonmethane hydrocarbons, values are from Figure 2.

^aB. Cros et al (unpublished manuscript, 1999).

^bT. Marion and P. Perros (unpublished manuscript, 1999).

^c*Delmas et al.* [this issue]

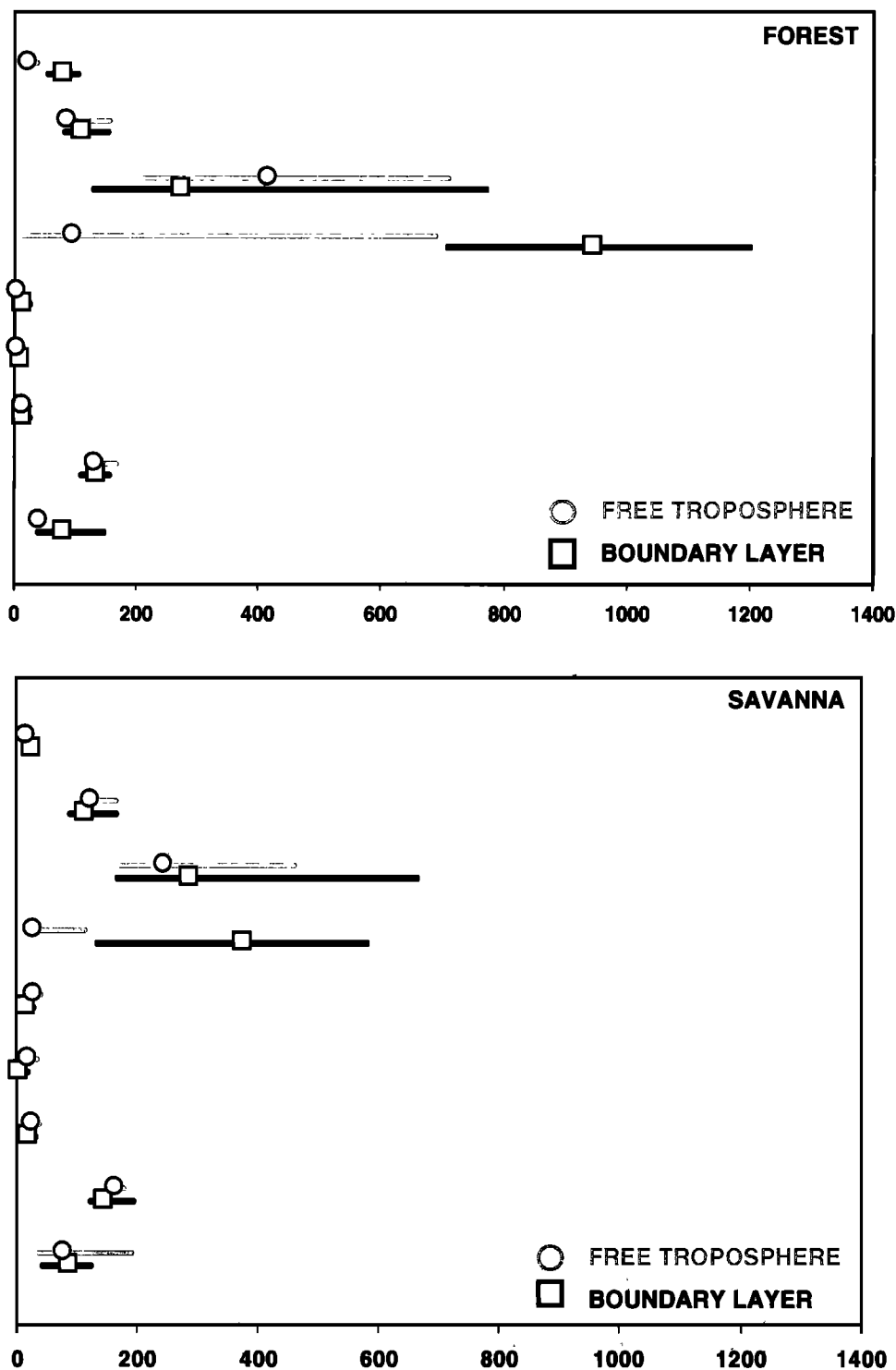


Figure 2. Concentrations (median and interquartile ranges) of several nonmethane hydrocarbons (NMHCs) in the boundary layer and free troposphere over the forest and transitional woodlands. Isoprene was the most abundant NMHC, despite extensive biomass burning activity several hundreds of kilometers upwind of the study region.

measured during the campaign. While the median mixing ratios of nonbiogenic VOCs were lower over the forest than the woodlands, the absolute differences between average values for individual flights over woodland or forest were small. Mixing ratios in the boundary layer and the free troposphere were very similar, indicating also that there was considerable exchange

between the boundary layer and the lower free troposphere. Finally, the trends in mixing ratios of nonbiogenic VOCs and CO were similar and may indicate the same distant source (most likely biomass burning).

CO and NMHC measurements were compared (Table 3) with those made during Transport and Atmospheric Chemistry near

Table 3. Comparison of Southern African (TRACE-A) and Central African (EXPRESSO) CO and Volatile Organic Compound Concentrations

		Boundary Layer ^a				
	Landcover	CO, ppb	C ₃ H ₈ , ppt	C ₃ H ₆	C ₆ H ₆ , ppt	Isoprene, ppt
TRACE-A	savanna	280	200	70	220	50-150
EXPRESSO	woodland	300	168	90	307	100-400
EXPRESSO	forest	285	126	72	267	710-1200
		Free Troposphere ^b				
TRACE-A	savanna	275	200	70	220	0-50
EXPRESSO	woodland	300	160	64	277	10-30
EXPRESSO	forest	290	143	41	193	20-300

Data for Transport and Atmospheric Chemistry near the Equator – Atlantic (TRACE-A) are from Blake et al. [1996]. EXPRESSO CO data are from C. Delon et al (unpublished manuscript, 1999).

^aSurface up to approximately 1000 m near midday.

^bFrom the top of the boundary layer to approximately 4 km in TRACE-A and EXPRESSO.

the Equator-Atlantic (TRACE-A) in southern Africa during its burning season [Blake et al., 1996]. Similar mixing ratios of NMHCs and CO (and CO/NMHC ratios) were seen over the savanna in both experiments. Lower VOC mixing ratios were measured during the EXPRESSO campaign over the forest, where mixing with cleaner monsoon maritime air, as well as increased aging of the biomass burning emissions, decreased average mixing ratios.

Isoprene and α -pinene were detected above the boundary layer (Figure 2) over the forest and the savanna (more over the forest). Blake et al. [1996] also reported isoprene concentrations of 50-150 ppt at the top of the boundary layer over the savanna; the concentrations dropped rapidly with higher altitude and were below the detection limit above 4 km.

3.2. REA Isoprene Fluxes

The results of REA flux measurements over the woodland and forest regions are displayed in Figure 3. The interquartile ranges of fluxes for forest and savanna are given, along with the interquartile range of latitudes over which they were measured. The median flux and latitude are at the intersection of the ranges. Medians are represented, instead of averages, since the measurements were not made to represent a normal distribution.

The REA fluxes were measured intensively over a primary and semideciduous rain forest near Enyele, Congo, and over transitional woodland near Boali, CAR (Plate 2). Most REA measurements were made at a height of approximately 100-200 m. Several forest REA measurements were made at

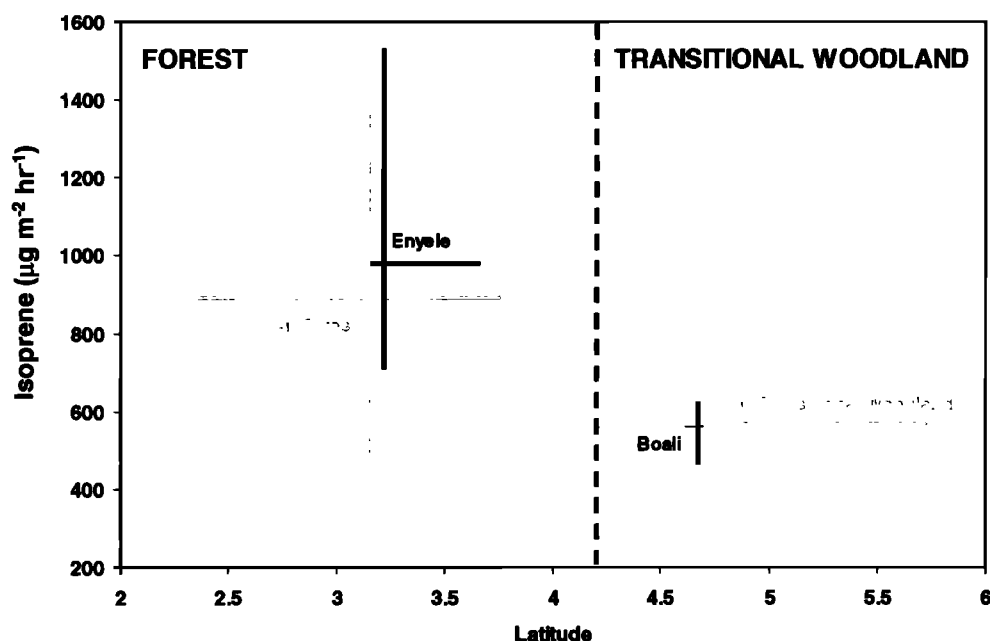


Figure 3. REA flux results. The vertical and horizontal bars represent the interquartile ranges of fluxes and latitudes over which REA flux measurements were made (these lines intersect at the median values). Most measurements were made over the Enyele forest and the Boali savanna sites (solid black lines); additional measurements from similar landscapes were included in the forest and transitional woodland averages (shaded lines).

approximately 600 m and may be less accurate, because of greater flux divergence higher in the mixed layer. Median REA isoprene fluxes (and interquartile range) were 980 (710-1530) and 560 (470-620) $\mu\text{g m}^{-2} \text{h}^{-1}$ for the Enyele rain forest and the Boali woodland, respectively, for REA samples collected below 200 m. The Enyele forest and the Boali woodland areas were indistinguishable in satellite observations from their respective surrounding landscapes. Consequently, all rain forest and transitional woodland measurements were combined, and REA median isoprene fluxes were calculated to be 890 (480-1540) and 570 (420-720) $\mu\text{g m}^{-2} \text{h}^{-1}$, respectively (Figure 3).

All of the REA measurements were made in the morning, most between 0930 and 1130. The maximum emissions for these landscapes likely occur in early afternoon, when temperature and light effects are at maximum levels. The measured emission fluxes are not normalized to any standard conditions (i.e., 30°C and 1000 $\mu\text{E m}^{-2} \text{s}^{-1}$ of photosynthetically active radiation, PAR), since species-specific emission algorithms for the roughly characterized landscapes are not known. However, during the November-December measurement period, average late morning temperatures measured at the airport in Bangui were 27°-30°C. Clear or mostly sunny skies prevailed during the morning flight hours, and PAR was likely greater than 1000 $\mu\text{E m}^{-2} \text{s}^{-1}$ (above approximately 800 $\mu\text{E m}^{-2} \text{s}^{-1}$ additional radiation has little effect on increasing isoprene emissions in species previously studied [Guenther *et al.*, 1995]).

The tropical forest and transitional woodland, over which REA measurements were made, are composed of several landscapes [Guenther *et al.*, this issue]. The forest area is categorized as semideciduous tropical forest and evergreen tropical rain forest. The transitional woodland contains primarily degraded secondary forest. These landscapes themselves, however, may contain a number of vegetation communities.

The REA flux measurements (Figure 3) are distributed over a range of values, greater over the forest areas. This range may be due, in part, to the species diversity within these landscapes. Other factors may also contribute to the measurement variability. The REA technique samples air only in eddies larger than a threshold determined by statistics of the vertical velocity measurements and by mechanical constraints (C. Delon *et al.*, unpublished manuscript, 1999). Consequently, a portion of the transport is not accumulated into the up and down reservoirs; this amount may be estimated from measurements of sensible heat flux, is typically less than 20% of the mass transport, and is considered in the flux calculation. Flux divergence may contribute some error, but this could not be quantified. All savanna REA samples were collected at altitudes less than 200 m. Uncertainties in the chromatographic analysis of isoprene concentration difference in the two reservoirs may also contribute errors of the order of 15%. The overall uncertainty of the flux measurements is estimated at 50% for the forest and 35% for the transitional woodland. Fluxes of terpenes were not computed for the REA method, since their concentrations were small (Figure 2) and the precision of the measurements was not sufficient. Fluxes of α -pinene in the morning hours were estimated from the model simulation (below) at 110 and 90 $\mu\text{g m}^{-2} \text{h}^{-1}$ from forest and woodland landscapes, respectively.

3.3. Comparison With Other Tropical VOC Flux Measurements and Estimates

Isoprene flux was measured by REA at the EXPRESSO tower in the N'doke Forest Reserve of the northern Congo (D. Serca *et*

al., unpublished manuscript, 1999). The tower was located within a tropical rain forest landscape. An average isoprene flux of 500 $\mu\text{g isoprene m}^{-2} \text{h}^{-1}$ was measured above the forest canopy in November 1996. A higher flux ($\sim 1100 \mu\text{g isoprene m}^{-2} \text{h}^{-1}$) was measured in March 1996. The difference in the November and March fluxes may be associated with seasonal effects during the dry and wet seasons, respectively. The November tower flux is at the lower end of the range of fluxes measured by the aircraft REA. However, the aircraft fluxes were measured over a variety of rain forest landscapes (a mosaic of tropical evergreen, edaphic, and seasonal forest communities). This may also explain the relatively large range of isoprene fluxes measured over the forest landscapes in the Congo, compared to the more narrow range of fluxes measured over the transitional forest/savanna region in the CAR, where the landscapes were more uniform (Plate 2).

Isoprene fluxes of approximately 4000 $\mu\text{g isoprene m}^{-2} \text{h}^{-1}$ have been reported for the a tropical evergreen rain forest in the Brazilian Amazon forest [Zimmerman *et al.*, 1988]. The species composition of African and South American rain forests is very different. Since isoprene emissions are species specific [Guenther *et al.*, 1995], differences in area emissions may be expected.

Guenther *et al.* [this issue] estimated emissions for these transitional woodlands and forests by integrating landscape biomass density with the emission capacity (the maximum emission rate at standard conditions) and emission activity factors (light, temperature, canopy position, seasonal effects, etc.), which modulate emissions) of vegetation species in the landscape. Emissions were estimated for the morning hours, when REA flux measurements were made. For times of day matching the REA measurements, the rain forest and transitional woodland landscapes were estimated to have isoprene emission rates of 1231 and 806 $\mu\text{g m}^{-2} \text{h}^{-1}$. The modeled results are higher than the median fluxes measured in situ by REA, but are within the uncertainty or ranges reported.

3.4. PBL Chemistry

The atmospheric chemistry over the EXPRESSO region during the November-December 1996 experimental period was influenced both by biomass burning in savanna areas to the north (P. A. Brivio *et al.*, unpublished manuscript, 1999) and the more local biogenic emissions from the savanna and forest areas. Average black carbon concentrations of about 10 $\mu\text{g m}^{-3}$ were measured from filter samples [Ruellan *et al.*, this issue], which along with high average CO and condensation nuclei (250-400 ppb and 2000-4500 particles cm^{-3} , respectively, (C. Delon *et al.*, unpublished manuscript, 1999)), O₃ (30-60 ppb, (B. Cros *et al.*, unpublished manuscript, 1999) and NO_x (250-400 ppb (T. Marion and P. Perros, unpublished manuscript, 1999)) strongly suggested the influence of biomass burning and the presence of absorbing aerosols. Concentrations of NMHCs associated with biomass burning, especially the more reactive VOCs, were relatively low compared to those in young plumes, presumably because of atmospheric reactions and dilution. Biogenic isoprene was the most abundant NMHC and also the most important reactive NMHC in the EXPRESSO savanna and forest regions (Figure 2). Since biomass burning and biogenic NMHC emissions are often associated with net O₃ production, the 0-D chemistry model was used to simulate the chemistry of the EXPRESSO boundary layer, focusing on photochemical oxidant chemistry in the savanna and forest environments.

Although the 0-D model has many limitations as further discussed below, the simulations demonstrate several aspects of

the photochemistry of the PBL. Perhaps the most important is the role of absorbing aerosols in controlling, through modification of photolysis rates, the overall reactivity of the PBL. Measurements of J_{NO_2} from aircraft (T. Marion and P. Perros, unpublished manuscript, 1999) show a marked decrease, by about a factor of 2, at the lower altitudes of the PBL, compared to free tropospheric altitudes. This J_{NO_2} gradient is observed even in the absence of clouds and can most plausibly be attributed to the presence of absorbing aerosols from biomass burning. In an aerosol-free troposphere (Rayleigh scattering only) and high Sun, the vertical gradient of J_{NO_2} would be much weaker than that observed, and scattering aerosols could even increase J_{NO_2} at lower altitudes [Dickerson *et al.*, 1997; Madronich and Flocke, 1998].

Figure 4 compares our calculations of J_{NO_2} and J_{O_3} with and without aerosols. At high Sun, a reduction of a factor of 2 in J_{NO_2} is attained by assuming an aerosol optical depth of about 1 at 550 nm (scaled spectrally by the inverse of wavelength), distributed vertically with the typical continental profile given by Elterman [1968], a wavelength-independent single-scattering albedo of 0.75, and an asymmetry factor of 0.61. Other choices of aerosol optical properties (not measured during the experiment) are possible, but insofar as our model inputs reproduce the observed factor of 2 reduction in J_{NO_2} , these would probably not alter our qualitative conclusions. The stronger reduction of J_{O_3} results from a combination of (1) the inverse wavelength scaling assumed for the aerosol optical depth and (2) the fact that photon path lengths in the UV-B region (of greater importance to J_{O_3}) are longer, at high Sun, than in the UV-A region (of importance to J_{NO_2}) due to greater Rayleigh scattering. Our assumption of higher aerosol optical depths at shorter wavelengths is also supported by recent measurements in polluted air masses [Wenny *et al.*, 1998].

The impact of photolysis rate reductions on isoprene, O_3 , and OH is illustrated in Table 4. The first row gives our more realistic reference case, which includes the reduction of J values by aerosols. The second row illustrates the effect of using aerosol-free J values. In this case, noontime OH concentrations are higher by more than a factor of 2, and isoprene concentrations fall well below the observed values. The impact of reduced

photolysis rates on ozone is more difficult to assess from Table 4, because the peak O_3 concentrations in the PBL are strongly influenced by entrainment of ozone-rich air (see below) during the growth of the PBL. We have estimated the net photochemical production of O_3 by subtracting the contributions of entrainment and surface deposition from the simulated total rate of ozone change $d[\text{O}_3]/dt$. For the reference case this analysis shows that net photochemical O_3 production occurs only during the central sunlit 5-6 hours of the day, peaking at about 6 ppb/h over the forest and 2 ppb/h over the savanna. When averaged over the entire day and integrated over the time-dependent height of the PBL, the local net photochemical O_3 production and deposition are roughly equal over the forest, while over the savanna deposition slightly exceeds local net photochemical production. The fact that the savanna PBL is a net ozone sink is a direct result of the suppressed photolysis rates, in combination with the high $\text{NO}_x/\text{hydrocarbon}$ ratio observed for that environment (see further discussion below).

A second interesting aspect of the 0-D model simulation arises from the different $\text{NO}_x/\text{hydrocarbon}$ ratios encountered in the savanna and forest boundary layers. The higher isoprene concentrations in the forest PBL lead to substantially lower OH values (see Table 4, reference case) compared to the savanna. However, the two regions have opposing sensitivities to changes in NO_x concentrations. It has long been recognized [e.g., Hameed *et al.*, 1979; Logan *et al.*, 1981] that at low $\text{NO}_x/\text{hydrocarbon}$ ratios, the further addition of NO_x leads to increases in O_3 and OH, while at higher ratios both OH and O_3 are suppressed. This latter situation occurs because the reaction $\text{OH} + \text{NO}_2 \rightarrow \text{HNO}_3$ competes against reactions of the type $\text{OH} + \text{hydrocarbons} + \text{O}_2 \rightarrow \text{RO}_2$, where the peroxy radicals (RO_2) would ultimately contribute to O_3 production. Increases in NO_x (see Table 4, third row) cause an increase in OH in the forest PBL, but decrease OH in the savanna PBL. Increases in isoprene lead to lower OH over the savanna and much lower OH over the forest (Table 4, fourth row). Changes in O_3 concentrations are rather small because, as already discussed above, the PBL O_3 levels are mostly determined by entrainment of free tropospheric air. It is also worth noting that the threshold $\text{NO}_x/\text{hydrocarbon}$ ratio (for the reversal of OH and O_3 production) is lower when

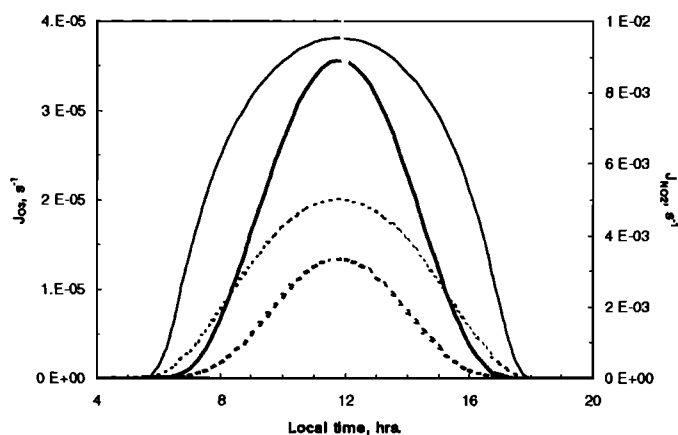


Figure 4. Photolysis rate coefficients (J values) for the reactions $\text{O}_3 + hv \rightarrow \text{O}_2 + \text{O}(^1\text{D})$ (heavy curves, left scale) and $\text{NO}_2 + hv \rightarrow \text{NO} + \text{O}(^3\text{P})$ (light curves, right scale), calculated with a delta-Eddington scheme for November 25, 1996 (latitude 4°N , 260 Dobson units, cloud-free, 0.5 km above a surface of 5% Lambertian reflectivity). Solid curves give values for aerosol-free conditions, dashed curves for aerosol visible range of 4 km (at 550 nm) with single-scattering albedo of 0.75.

Table 4. Sensitivity of Boundary Layer Photochemistry to Parameters in Zero-Dimensional Model

Case	Savanna			Forest		
	Isoprene ^a , ppbv	O ₃ ^b ppbv	OH, ^c 10 ⁶ molecules cm ⁻³	Isoprene, ppbv	O ₃ , ppbv	OH, ^c 10 ⁶ molecules cm ⁻³
Reference	0.2-0.8 ^a	53 ^b	4.8 ^c	0.9-2.0	48	5.5
Increased <i>J</i> ^d	0.1-0.2	60	12	0.3-0.5	53	7.5
Double NO _x	0.3-1.0	53	4.1	0.8-2.0	51	4.2
Double isoprene	0.6-1.7	55	3.8	2.7-4.3	49	1.6
Increased <i>J</i> and doubled NO _x	0.1-0.3	64	16	0.2-0.5	64	14
Increased <i>J</i> , doubled Isoprene	0.2-0.5	62	10	1.5-1.8	54	3.3
Decreased isoprene deposition velocity from 0.1 to 0 cm/s	0.2-0.9	54	4.8	0.9-2.2	48	3.0
Increased O ₃ deposition velocity from 0.5 to 2 cm/s	0.2-0.9	49	4.3	0.8-2.0	41	3.3

^aIsoprene evaluated between about 0930 am (higher value) and noon (lower value).

^bO₃ maximum, occurring in early afternoon.

^cOH maximum, occurring near noon.

^dPhotolysis increased to represent aerosol-free conditions.

photolysis rate coefficients are lower, as is the case here due to the effects of absorbing aerosols. If *J* values are hypothetically increased to aerosol-free values, doubling of NO_x results in strong OH increases (compare second and fifth rows of Table 4), while doubling of isoprene decreases OH (compare second and sixth rows), in both forest and savanna PBLs. Some additional PBL O₃ production would also occur. Thus the reduction in *J* values by aerosols does not simply scale the magnitude of photochemical processing, but also changes the qualitative NO_x/hydrocarbon regime of both PBLs.

A third result highlights the limitations of the 0-D model in simulating the vertical structure of PBL mixing. Diurnal variations of isoprene concentration in the PBL result from the assumed time dependence of isoprene emissions, from reactions with OH, O₃, and NO₃, and also from the assumed vertical variations of the PBL height. A sharp decrease of isoprene concentrations computed in the late morning is due mainly to the rapid growth of the PBL, while the sharp isoprene rise in the late afternoon is associated with emissions into a shrinking PBL volume. Since aircraft isoprene measurements (seven integrated 10-15 min samples) were made during, at most, a 75-min period during each flight, this pattern was not observed in individual flights and could not be validated from combining the data of several flights. However, the daytime pattern has been described for isoprene from tethered balloon measurements in the boundary layer [Greenberg *et al.*, 1999]; those data indicate relatively constant isoprene concentrations in the mixed layer around midday.

The calculated PBL O₃ concentrations (see Table 4, reference case) are substantially higher than those measured (see Table 2). The reason for this overestimate is related less to photochemical O₃ production in the PBL than to the assumed rapid entrainment of O₃-rich background air as the PBL top height rises. Any 0-D model assumes inherently that all chemical concentrations are instantly and completely mixed through the PBL. This overestimate of actual vertical mixing may be particularly serious in the presence (as already noted) of strongly absorbing aerosols which may cause complex vertical heating profiles and therefore further barriers to mixing [Raga *et al.*, 1998]. The latter problem

may prove challenging even for multidimensional models, if detailed aerosol processes are not modeled on appropriately fine spatial scales.

Finally, organic peroxy radicals (RO₂, see Figure 5) computed by the model are highly illustrative of the overall photochemical activity in the PBL. The midday peak is associated mainly with isoprene oxidation by the OH radicals produced under high solar irradiation, with some contribution from the reaction of O₃ with isoprene, and OH with methane and other nonmethane hydrocarbons. The large peak at dusk, which was observed in all simulations, is due to the reaction of NO₃ radicals with isoprene and is enhanced by slower nighttime losses of the resulting organic peroxy radicals (because of lower NO). The timing of this peak is highly predictable, as substantial NO₃ concentrations cannot be sustained during sunlit hours, while the available reagents (isoprene and NO_x) decrease rapidly at night due to their destructive interaction, as well as reduced emissions. In separate simulations, setting the rate constant for the NO₃ + isoprene reaction to zero eliminated the dusk RO₂ peak and resulted in considerably slower evening decay of isoprene concentrations. On the other hand, setting either isoprene or O₃ deposition velocities to zero had only a minor effect on concentrations (see Table 4).

In our simulations the reaction NO₃ + isoprene was the main reason for the decrease in isoprene concentrations seen in the early evening hours. These losses have been previously explained by isoprene deposition [Jacob and Wofsy, 1988; Cleveland and Yavitt, 1997]. More recently, the nighttime isoprene loss has also been attributed to its reaction with NO₃ radicals in high-NO_x and high-O₃ environments [Starn *et al.*, 1998].

4. Summary and Conclusions

The EXPRESSO experiment focused on the atmospheric chemistry over the woodlands and forests of the Central African Republic and the Republic of the Congo during the biomass burning season. Burning activity was intense in areas influencing the region, as seen from satellite fire observations. The most intense burning activity, however, was several hundred

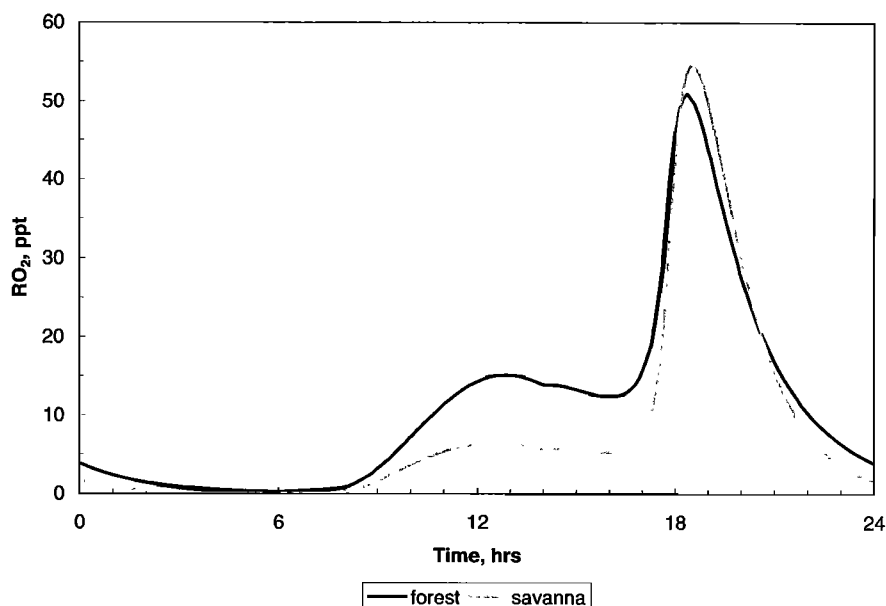


Figure 5. Concentrations of organic peroxy radicals (RO_2) computed with the zero-dimensional model (reference case of Table 4).

kilometers from the area of the aircraft measurements. NO_x , NO_y , and CO , and as well as aerosols, were observed at high levels characteristic of burning. Nonmethane hydrocarbons, except for isoprene, however, were at low concentrations (measured from 100 to 4000 m above the surface), which suggested that the air studied in the EXPRESSO region was a well-aged biomass burning plume. The concentrations of many of these gases and aerosols were expected to increase in the EXPRESSO region as the burning activity moved further south with the dry season.

Local biogenic emissions of isoprene provided the dominant reactive hydrocarbon in the atmospheric boundary layer in both the forest and woodland (savanna) regions studied (700–1000 and 100–400 ppt, respectively). The PBL concentration of α -pinene, another emission from vegetation, was in the range of 30–100 and 20–30 ppt over the same landscapes. Isoprene fluxes from the forest and woodland landscapes were measured directly aboard the aircraft by a relaxed eddy accumulation technique. Isoprene emissions were 890 and 570 $\mu\text{g m}^{-2} \text{h}^{-1}$ from forest and woodland landscapes, respectively, in the morning hours; these emissions correspond to daily emissions of 10.6 and 6.5 $\text{mg isoprene m}^{-2} \text{d}^{-1}$, for forest and woodland landscapes, respectively. The daily isoprene flux from the forest was more than a factor of 2 lower than reported for the Amazon tropical forest, also at the beginning of the burning season [Zimmerman *et al.*, 1988]. These emissions, as well as ambient isoprene concentrations, may change seasonally, depending on the phenology of individual emitting species. The flux of isoprene measured during the wet season at the EXPRESSO tower in the northern Congo was approximately 2 times that measured in November at the beginning of the dry (burning) season.

The aircraft measurements were used in a 0-D simulation of the chemistry. The simulation used measured isoprene emission fluxes to reproduce measured ambient isoprene concentrations. The photolysis rates measured during the campaign were consistent with significant aerosol UV radiation absorption, so that J_{NO_2} and J_{O_3} were reduced to approximately one half of clear sky values. Lower photolysis rates influenced the resulting

photochemistry. Both O_3 production and OH concentrations were reduced in the PBL compared to clear sky conditions. The forest and savanna regions had different sensitivities to changes in NO_x , so that the NO_x /hydrocarbon ratios from increased emissions of NO_x or isoprene had different effects on O_3 production and OH concentrations. While net O_3 production in the boundary layer (the domain of the simulation) was small, extensive mixing between the monsoon (boundary) and Harmattan (free troposphere) layers could enhance large-scale O_3 production, because of the export of precursors including unreacted hydrocarbons and partly oxygenated and nitrogenated intermediates. This net O_3 production has not been reported from satellite observations, possibly because of the rapid dilution effects in the Hadley and Walker circulation near the ITCZ (the region studied). This contrasts with the results from the Southern African Fire-Atmosphere Research Initiative (SAFARI)-TRACE-A experiment, where meteorological conditions recirculate air over southern Africa during the dry season, allowing for the observed high concentrations of O_3 to be produced over southern Africa.

The model simulation also indicated the importance of NO_3 chemistry in the rapid destruction of isoprene in the hours immediately surrounding sunset. This phenomenon has been observed in high- NO_x and high- O_3 environments, where isoprene concentrations decline rapidly after sunset to a few percent of daytime concentrations. The disappearance of isoprene at sunset is also accompanied in the simulation by a large production of organic peroxy radicals (RO_2) derived from isoprene oxidation. The predictable timing and high peak RO_2 concentration make it a good candidate for detection, which, however, to our knowledge has not been reported.

Acknowledgments. We thank P.R. Zimmerman for his contributions to the development of the EXPRESSO program. We also wish to thank the Institut Géographique National and the Institut National des Sciences de l'Univers, who organized and executed the operation of ARAT during the EXPRESSO campaign. The National Center for Atmospheric Research is sponsored by the National Science Foundation.

References

- Andreae, M.O., A. Chapuis, B. Cros, J. Fontan, G. Helas, C. Justice, Y.J. Kaufman, A. Minga, and D. Nganga, Ozone and Aitken nuclei over equatorial Africa: Airborne observations during DECAFE 88, *J. Geophys. Res.*, **97**, 6137-6148, 1992.
- Aumont, B., S. Madronich, M. Ammann, E. Baltensperger, D. Hauglustaine, and F. Brocheton, On the $\text{NO}_2 + \text{soot}$ reaction in the atmosphere, *J. Geophys. Res.*, **104**, 1729-1736, 1999.
- Blake, N.J., D.R. Blake, B.C. Sive, T.-Y. Chen, and F.S. Rowland, Biomass burning emissions and vertical distribution of atmospheric methyl halides and other oxidized carbon gases in the South Atlantic region, *J. Geophys. Res.*, **101**, 24,151-24,164, 1996.
- Brasseur, G., E. Atlas, D. Erickson, A. Fried, J. Greenberg, A. Guenther, P. Harley, E. Holland, L. Klinger, B. Ridley, and G. Tyndall, Trace gas exchanges and biogeochemical cycles, in *Atmospheric Chemistry and Global Change*, edited by G. Brasseur, J. Orlando, and G. Tyndall, pp. 189-242, Oxford Univ. Press, New York, 1999.
- Cachier, H., and J. Drucet, Influence of biomass burning on equatorial African rain, *Nature*, **352**, 228-230, 1991.
- Cleveland, C.C., and J.B. Yavitt, Consumption of atmospheric isoprene in soil, *Geophys. Res. Lett.*, **24**, 2379-2382, 1997.
- Crutzen, P.J., and M.O. Andreae, Biomass burning in the tropics: Impact on atmospheric chemistry and biogeochemical cycles, *Science*, **250**, 1669-1678, 1990.
- Delmas, et al., R.A. Experiment for Regional Sources and Sinks of Oxidants (EXPRESSO): An overview, *J. Geophys. Res.*, this issue.
- Dickerson, R. R., S. Kondragunta, G. Stencikov, K. L. Civerolo, B. G. Doddridge, and B. N. Holben, The impact of aerosols on solar ultraviolet radiation and photochemical smog, *Science*, **278**, 827-830, 1997.
- Dwyer, E., J.-M. Gregoire, and J.-P. Malingreau, A global analysis of vegetation fires using satellite images: Spatial and temporal dynamics, *Ambio*, **27**(3), 175-181, 1998.
- Elterman, L., UV, visible, and IR attenuation for altitudes to 50 km, Rep. 68-0153, Air Force Cambridge Res. Lab., Cambridge, Mass., 1968.
- Greenberg, J.P., B. Lee, D. Helmig, and P.R. Zimmerman, Fully automated gas chromatograph-flame ionization detector system for the in situ determination of atmospheric non-methane hydrocarbons at low parts per trillion concentration, *J. Chromatogr. A*, **676**, 389-398, 1994.
- Greenberg, J.P., D. Helmig, and P.R. Zimmerman, Seasonal measurements of non-methane hydrocarbons and carbon monoxide at the Mauna Loa Observatory during the Mauna Loa Photochemistry Experiment 2, *J. Geophys. Res.*, **101**, 14,581-14,598, 1996.
- Greenberg, J.P., A. Guenther, P. Zimmerman, W. Baugh, C. Geron, K. Davis, D. Helmig, and L.F. Klinger, Tethered balloon measurements of biogenic VOCs in the atmospheric boundary layer, *Atmos. Environ.*, **33**, 855-867, 1999.
- Guenther, A. et al., A global model of natural volatile organic compound emissions, *J. Geophys. Res.*, **100**, 8873-8889, 1995.
- Guenther, A., L. Otter, P. Zimmerman, J. Greenberg, R. Scholes, and M. Scholes, Biogenic hydrocarbon emissions from southern African savanna, *J. Geophys. Res.*, **101**, 25,859-25,865, 1996.
- Guenther, A., B. Bauth, G. Brasseur, J. Greenberg, P. Harley, L. Klinger, D. Serca, and L. Vierling, Isoprene emission estimates and uncertainties for the central African EXPRESSO study domain, *J. Geophys. Res.*, this issue.
- Hameed, S., J. P. Pinto, and R. W. Stewart, Sensitivity of the predicted CO-OH-CH_4 perturbation to tropospheric NO_x concentrations, *J. Geophys. Res.*, **84**, 763-768, 1979.
- Hao, W.M., and M.H. Liu, Spatial and temporal distribution of tropical biomass burning, *Global Biogeochem. Cycles*, **8**, 495-503, 1994.
- Jacob, D.J., and S. Wofsy, Photochemistry of biogenic emissions over the Amazon forest, *J. Geophys. Res.*, **93**, 1477-1486, 1988.
- Klinger, L.F., J. Greenberg, A. Guenther, G. Tyndall, P. Zimmerman, M. M'Bangui, J.-M. Moutsambote, and D. Kenfack, Patterns in volatile organic compound emissions along a savanna-rain forest gradient in central Africa, *J. Geophys. Res.*, **103**, 1443-1454, 1998.
- Lenschow, D.H., The use of aircraft for probing the atmospheric boundary layer, in *Atmospheric Technology*, pp. 44-49, Natl. Cent. for Atmos. Res., Boulder, Colo., 1975.
- Logan, J. A., M. J. Prather, S. C. Wofsy, and M. B. McElroy, Tropospheric chemistry: A global perspective, *J. Geophys. Res.*, **86**, 7210-7254, 1981.
- Lopez, A., M.L. Huertas, and J.M. Lacombe, Numerical simulation of the ozone chemistry observed over forested tropical areas during DECAFE experiments, *J. Geophys. Res.*, **97**, 6149-6158, 1992.
- Madronich, S., and J. G. Calvert, Permutation reactions of organic peroxy radicals in the troposphere, *J. Geophys. Res.*, **95**, 5697-5715, 1990.
- Madronich, S., and S. Flocke, The role of solar radiation in atmospheric chemistry, in *Handbook of Environmental Chemistry*, edited by P. Boule, pp. 1-26, Springer-Verlag, New York, 1998.
- Raga, G., D. Baumgardner, and J. Ogren, The direct radiative forcing by Mexico City aerosols on downwind climate, paper presented at 9th Symposium of the IAMAS Commission on Atmospheric Chemistry and 5th Scientific Conference of the International Global Atmospheric Chemistry Project, Seattle, Wash., Aug. 19-25, 1998.
- Rodin, L.E., N.I. Bazilevich, and N.N. Rozov, Productivity of the world's main ecosystems, in *Productivity of the World Ecosystem: Proceedings Seattle Symposium 1974*, edited by D.E. Reichle, pp. 13-26, Nat. Acad. of Sci., Washington, D.C., 1975.
- Ruellan, S., H. Cachier, A. Gaudichlet, P. Masclet, and J.P. Lacaux, Airborne aerosols over central Africa during the EXPRESSO experiment, *J. Geophys. Res.*, this issue.
- Starn, T.K., P.B. Shepson, S.B. Bertman, D.D. Riemer, R.G. Zika, and K. Olszyna, Nighttime isoprene chemistry at an urban-impacted forest site, *J. Geophys. Res.*, **103**, 22,437-22,447, 1998.
- Wenny, B.N., J. S. Schafer, J. J. DeLuise, V. K. Saxena, W. F. Barnard, I. V. Petropavlovskikh, and A. J. Vergamini, A study of regional aerosol radiative properties and effects on ultraviolet-B radiation, *J. Geophys. Res.*, **103**, 17,083-17,097, 1998.
- Wesely, M.L., Parameterization of surface resistance to gaseous dry deposition in regional-scale numerical models, *Atmos. Environ.*, **23**, 1293-1304, 1989.
- Zimmerman, P.R., J.P. Greenberg, and C. Westberg, Measurements of atmospheric hydrocarbons and biogenic emission fluxes in the Amazon boundary layer, *J. Geophys. Res.*, **93**, 1407-1416, 1988.

W. Baugh, J. P. Greenberg, A. B. Guenther, and S. Madronich, National Center for Atmospheric Research, Atmospheric Chemistry Division, 1850 Table Mesa Drive, Boulder, CO 80307. (e-mail: greenber@ucar.edu)

R. Delmas, C. Delon, and A. Druilhet, Laboratoire d' Aerologie, OMP, 14 Avenue Edouard Belin, 31 400 Toulouse, France.

P. Ginoux, NASA Goddard Space Flight Center, Code 916 Greenbelt, MD 20771

(Received May 5, 1999; revised June 21, 1999; accepted June 30, 1999.)